Proc. II World Conference on Experimental Heat Transfer, Fluid Mechanics and Thermodynamics, Dubrovnik, Yugoslavia, 1991, pp. 1267 - 1274

TURBULENT HEAT TRANSFER IN A RECTANGULAR DUCT WITH A MULTIPLE-SWIRL JET INLET CONDITION

A.C.R. Nogueira and L.F.A. Azevedo

Department of Mechanical Engineering
Pontifícia Universidade Católica do Rio de Janeiro
22453 - Rio de Janeiro, Brazil

ABSTRACT

The heat transfer characteristics of turbulent swirling flows through a low aspect ratio rectangular duct were investigated experimentally. A swirl generating section formed by several parallel twisted tapes, installed at the inlet plane of the duct provided the desired initial flow condition. Local and average heat transfer coefficients were determined by the utilization of the naphthalene sublimation technique in conjunction with the analogy between heat and mass transfer. Local results were provided along the whole active surface of the duct utilizing a fully automated coordinate table and depth gage. The study encompassed the investigation of the local heat transfer coefficient distribution for three values of the duct Reynolds number and for three values of the swirl intensity given by different tape pitch-to-diameter ratios. The results showed regions of high heat transfer augmentation, when compared to the base case results characterized by turbulent flow through a duct without the swirl flow inlet condition.

INTRODUCTION

This paper is concerned with the study of the heat transfer characteristics of turbulent swirling flows through a rectangular duct of low aspect ratio. To better understand the configuration investigated, reference is made to Figure 1. The figure shows a view of the inlet portion of a rectangular duct, where secondary motions imposed on the main axial flow are represented by a system of counterrotating vortices. These vortices are created by vortex generators positioned outside the duct (not shown in the figure), and are expected to decay as the flow proceeds along the axial direction. The objective of the present work is to provide information on the effects of this swirl flow inlet condition on the heat transfer from the principal wall of the duct.

The motivation for this study comes from the expectation that the swirling flow inlet condition just described will enhance the heat transfer from the duct walls. Systems of longitudinal vortices appear naturally as a result of flow instabilities in situations such as corrugated channels [1], inclined channels in natural convection [2], and mixed convection in horizontal ducts [3]. In all these cases, heat transfer augmentation was observed and related to the presence of such vortex motion. Although the physical mechanisms which are responsible for the presence of the vortex system in the configurations mentioned are quite diverse from the present situation, it is conceivable that similar augmentation effects could be obtained by the utilization of externally induced swirling inlet conditions. The magnitude of the heat transfer increase and its rate of decay along the duct length, are important information which will be provided by the present study.

Forced convection heat transfer in rectangular ducts has been the objective of several experimental and numerical investigations (e.g., [4]). Swirling flows have also been extensively studied for the circular duct geometry (e.g. [5]). However, an extensive literature search conducted failed to reveal any previous work dealing with swirling flows through rectangular ducts, despite its potential for heat transfer augmentation.

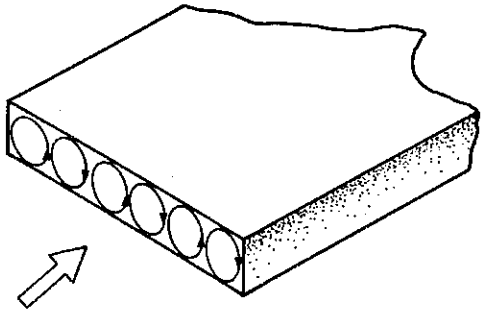

Fig. 1 - Schematic view of the swirl flow configuration studied.

EXPERIMENTS

The expected spanwise variation of the heat transfer coefficient resulting from the inlet conditions employed in the present study, required the utilization of a measuring technique capable of providing local measurements of these coefficients. The heat transfer results to be presented here were obtained by the utilization of mass transfer experiments in conjunction with the analogy between the heat and mass transfer processes. The naphthalene sublimation technique was employed since it is a well established method known to produce accurate average and local results, for the analog of a constant wall temperature boundary condition [6]. The test section and measuring system constructed will now be described.

Figure 2 shows a schematic view of the test section. Air, from a temperature controlled laboratory room, was drawn into the test section by a blower positioned outside the laboratory building. The air passed through a swirl generating section, traversed the length of a flat rectangular channel, passed through an orifice plate flow meter, a control valve, and was finally exausted to the outside ambient. A transition chamber was used to provide the matching from the rectangular duct cross section to the circular cross section of the pipe conduting the air to the blower.

Rectangular Channel. The flat rectangular channel was the main part of the test section, and was formed by two principal walls and two side walls. The internal dimensions of the duct were 14.7 x 145.0 x 1650 mm (height x width x

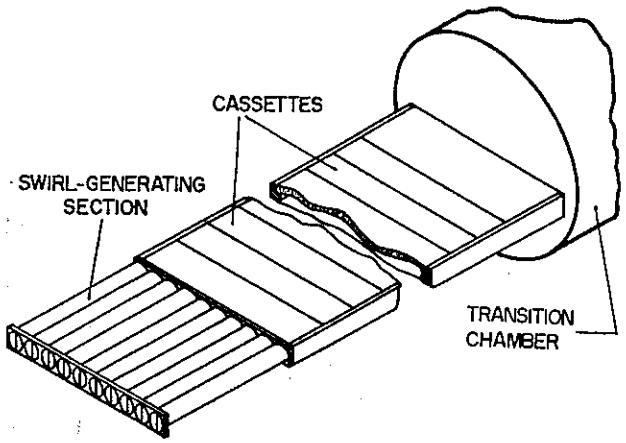

Figure 2. Schematic view of the test section.

length), yielding a duct cross-sectional aspect ratio (width / height) of about 10. A polished aluminum plate served as the lower principal wall of the duct, thereby providing an inert surface as far as naphthalene sublimation is concerned. This inactive surface represents in the mass transfer experiments the analog of an adiabatic wall in a heat transfer experiment. One aluminum bar was fixed along each edge of this aluminum plate. These bars served as the side walls of the duct and displayed recesses machined along their inner upper edges, provided in order to mate with the upper principal wall, as indicated in Figure 3(a).

The upper wall was the active surface of the channel. It was formed by 30, 5 x 150 x 50 mm (thickness x width x length) aluminum cassettes, precisely machined to the shape shown in Figure 3(a). The empty space of these C-shaped cassettes was filled with solid naphthalene by a casting pro cess which will shortly be described. The lateral edges of the cassettes rested on the recesses machined on the side walls of the duct. Once assembled in the rectangular duct, the 30 cassettes formed a perfectly continuous naphthalene surface which constituted the upper principal wall of the duct. The remainder of the duct length not covered by the 30 cassettes was completed by a solid aluminum plate fixed into the recesses on the edges of the side walls. The dimensions of each cassette were determined having in mind two limitations of the measuring equipment, namely, the maximum weight allowed by the precision balance available for the average mass transfer measurements, and the maximum travel of the automated coordinate table utilized for the local measurements.

Sealing of the duct was achieved by covering the external surfaces of the cassettes mounted in the test section with a rubber sheet. A 5 mm-thick aluminum plate having the same dimensions as the test section was then placed over the rubber sheet and pressed down by 24 fast-release clamps. Part of the assembled rectangular duct is shown schematically in Figure 3(b). The first cassette, which was positioned at the duct entrance, was specially machined so as not to allow that the lateral naphthalene surface be exposed to the air entering the duct which, otherwise, would produce unwanted naphthalene sublimation (see Figure 3(a)).

For comparison purposes, mass transfer experiments were also performed for the case of developing flow in a rectangular duct without the inlet swirl condition. In this situation, a 500 x 500 mm square baffle plate was installed at the inlet plane of the duct. The plate, having a opening that perfectly matched the cross-sectional shape of the rectangular duct, served to define the inlet flow condition.

Swirl-Generating Section. The swirl flow inlet condition utilized in the experiments was obtained by the utilization of a swirl-generating section formed by ten 14.7 x 500 mm (internal diameter x length) copper tubes parallel to each other, with twisted tape inserts. The internal diameter of the tubes was exactly of the same dimension as the height of the rectangular channel, thereby providing a smooth transition for the flow leaving the tubes and penetrating into the rectangular channel. The tubes were held together by soldering them to copper end plates previously machined to accommodate the cross sectional shape of the set of tubes. One of the end plates served to fix the swirl-gerating section to the rectangular duct inlet plane.

The twisted tapes were fabricated from 1-mm-thick galvanized steel strips with lateral dimensions which provided a snug fit to the inner wall of the copper tubes. Special care was taken during the twisting of the steel strips, to ensure that the ten twisted tapes fabricated would display the same pitch. This was an important requirement since a nonuniform swirl flow condition might have resulted from the utilization of tapes in the swirl-generating section with different pitches. An excellent uniformity on the pitch of the tapes fabricated was obtained by twisting them under constant tension in an INSTRON universal testing machine. The pitch uniformity was verified by measurement performed by a caliper with a special attachment installed at its measuring tips. Tapes with the three following pitch-to-diameter ratios, P/D, were fabricated: 22.0, 10.3, and 4.4. Tapes with smaller pitch-to-diameter ratios could not have been fabricated due to tape buckling failure. Left and right handed twisted tapes were fabricated for each value of the pitch-to-diameter ratio. These two types of tapes allowed the realization of the desired counterrotating swirl condition at the rectangular duct inlet plane.

Casting Process. The C-shaped aluminum cassettes to be filled with naphthalene were positioned on a stainless steel surface and firmly fixed to it by clamps. One stainless steel

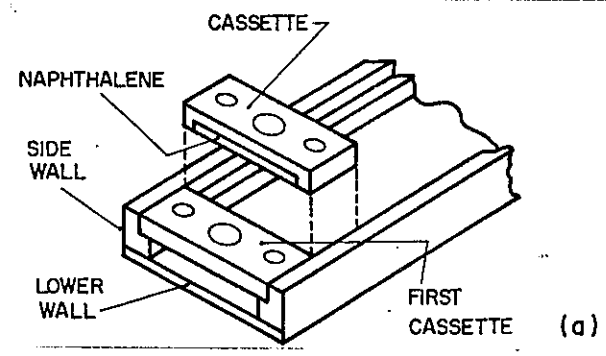

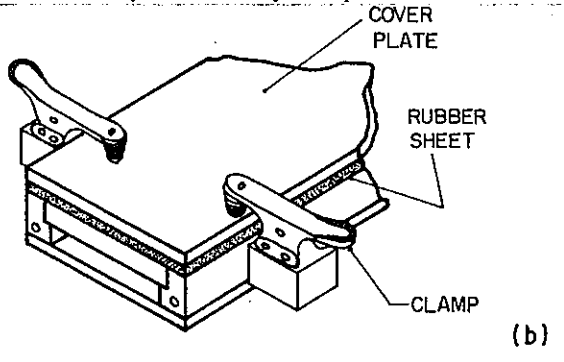

Fig. 3. Detailed view of the inlet portion of the rectangular duct.

bar was positioned at each side of the cassette, thereby forming a cavity for the casting operation. As can be seen in Figure 3(a), three holes were provided on the upper surface of the cassettes. Liquid naphthalene was introduced into the mould through the central hole, while the lateral ones served as vents for the air trapped in the mold. The highly polished finish of the stainless steel surfaces utilized guaranteed an excelent finish for the naphthalene surface produced by the casting operation. The pouring and the vent holes were then covered with wax to avoid undesired naphthalene sublimation. Special care was taken to guarantee that the covering wax did not protude from the cassette back surface. This was necessary since during the local measurements this surface rested on the flat surface of the coordinate table.

One of the cassettes was instrumented with a teflon-coated chromel-constantan thermocouple (0.127-mm diameter) with the objective of monitoring the naphthalene surface temperature during the data runs. The thermocouple was introduced in one of the vent holes before the filling of the mold, and maintained in contact with the stainless steel plate until the solidified naphthalene would secure it in position.

Measuring System. Two kinds of measurements were performed in the experiments conducted. Cassette-averaged mass transfer coefficients were obtained by weighing the naphthalene-filled aluminum cassttes in a precision balance, before and after they were exposed to the air flow in the test section. A Sartorious analytic balance with a resolution of 10^{-4} grams was utilized in these measurements.

Spanwise and axial variations of the mass transfer coefficients induced by the swirl flow inlet condition were investigated by local measurements. This was achieved by measurements of the contour of the naphthalene test surfaces conducted before and after a data run. The difference in elevation at a particular position yields the depth of sublimation, which is related to the local mass transfer coefficient. Since one of the objectives of the work was to provide information on the rate of decay of the induced swirl flow, local measurements had to be performed for large values of the axial coordinate, i.e., for a great number of cassettes. It was readily seen that the investigation of local transfer coefficients over such an extense area was only feasible by the utilization of a computer-assisted data acquisition system.

The data acquisition system constructed consisted of a stationary depth gage mounted on a precision coordinate table, over which the cassette to be measured was positioned with the naphthalene surface facing up. The coordinate table was formed by two single-axis tables, perpendicularly mounted. Precise positioning was achieved by the utilization of zero-backlash lead-screws and zero-radial clearence linear bearings produced by EGROJ Industrial and RPL Rolamentos Paulistas, respectively. The coordinate table was driven by two stepper motors and controllers from Syncro Industrial, which were capable of providing 500 steps/revolution, with a noncumulative error of 3% per step increment. The maximum travel allowed for the table in each orthogonal direction was of the order of 200 mm, with a positioning accuracy of about 0.05 mm.

The depth gage and signal conditioner used to survey the naphthalene surface were made by Diadur, and presented a resolution of the order of 0.5 μm. The coordinate table and the depth gage comunicated by a specially designed interface to a PC-XT compatible computer which controlled the measuring process and reduced the acquired data. In a typical measuring operation 1000 points were visited over the cassette naphthalene surface, taking aproximately 20 minutes for data acquisition and storage.

Experimental Procedure. Prior to data run, the solid naphthalene from the cassettes utilized in the previous run were melted and evaporated. Unused naphthalene was then employed in the casting of a new set of cassettes. After the casting operation, the cassettes were wraped in aluminum foil to avoid undesired sublimation, and taken to the temperature controlled laboratory room for a period of 24 hours to attain thermal equilibrium. The naphthalene filled cassettes were weighted in the precision balance and taken to the measuring coordinate table for the pre-data run surface contour measurements. The weighing operation was executed even when only local measurements were to be performend. As will be seen shortly, this total weight information was utilized to check the correctness of the local measurements obtained from the coordinate table, by comparing it to the integrated local results.

The cassettes were then mounted in the test section, which has been previously warmed up and pre-set at the air mass flow rate of the particular case being studied. After the test period, the cassettes were removed, wraped in aluminum foil and the measurements in the balance and coordinate table repeated.

To facilitate the precise positioning of the cassettes on the coordinate table, two guide bars were bolted to the measuring surface. These guides, mounted at ninety degrees, served to guarantee the return of the cassette to the same position as in the pre-data run measurements. During the mapping of the naphthalene surface, the elevation of three points situated on the exposed aluminum part of the cassettes were also recorded. These values served to calculate a datum plane to which all naphthalene measurements were referenced.

The air run time in each experiment was defined by two factors. It is highly desirable, from the stand point of the measurement uncertainties, that the depth of sublimation (or the total mass sublimed) be large. On the other hand, large depths of sublimation produce undesired distortions of the naphthalene test surface. Auxiliary runs were performed for each value of the channel Reynolds number investigated to select a proper run time. Typically, sublimation depths were kept within the 40-120 μm range.

Data Reduction. The calculation of the local mass transfer coefficient distribution required the knowledge of the depth of sublimation distribution $\delta(x,y)$, where x and y are the streamwise and spanwise coordinates, respectively. This was obtained by differencing the elevation at each (x,y) point on the naphthalene surface measured after and before the data run. Then the local mass transfer per unit surface area, $\dot{m}''(x,y)$, can be calculated as

$$\dot{m}''(x,y) = \rho_s \delta(x,y)/\Delta t \qquad (1)$$

where ρ_s is the density of the solid naphthalene (1.146 g/cm^3) and Δt is the duration time of the data run. The local mass transfer coefficient is defined as

$$K(x,y) = \frac{\dot{m}''(x,y)}{\rho_{nw} - \rho_{nb}(x)} \qquad (2)$$

where ρ_{nw} and $\rho_{nb}(x)$ stand, respectively, for the naphthalene vapor densities at the wall and in the bulk of the fluid, at a particular axial position. The bulk density can be calculated by integrating the mass of naphthalene sublimed to the air from the begining of the duct up to the axial position of interest. Assuming a constant air volume flow rate $\dot{Q}$, a mass balance yields

$$\rho_{nb}(x) = \frac{1}{\dot{Q}} \int_0^x \dot{M}''(x)dx \qquad (3)$$

In the above equation, $\dot{M}''(x)$ is the spanwise-averaged mass transfer calculated as

$$\dot{M}''(x) = \frac{1}{w}\int_0^w \dot{m}''(x,y)dy \qquad (4)$$

The Sogin vapor pressure-temperature relation [7] and the perfect gas law were employed to calculate ρ_{nw}, using the surface temperature measured with the thermocouple flushed mounted with the naphthalene surface, as described earlier.

In the presentation of the results, the spanwise-averaged transfer coefficients were also employed. They were calculated as

$$\bar{K}(x) = \frac{\dot{M}''(x)}{(\rho_{nw} - \rho_{nb}(x))} \qquad (5)$$

Cassette-averaged mass transfer coefficients were calculated from the balance measurements by

$$\bar{K}_c = \frac{\Delta m/(A\Delta t)}{\text{Log mean } \Delta\rho_n} \qquad (6)$$

In equation (6), Δm is the overall mass transfer obtained from before and after weighings of a naphthalene-filled cassette, A is the exposed naphthalene surface area, and the log mean density difference is defined as

$$\text{Log mean } \Delta\rho_n = \frac{(\rho_{nw} - \rho_{nb,i}) - (\rho_{nw} - \rho_{nb,e})}{ln\left((\rho_{nw} - \rho_{nb,i})\,/\,(\rho_{nw} - \rho_{nb,e})\right)} \qquad (7)$$

where $\rho_{nb,i}$ and $\rho_{nb,e}$ are, respectively, the bulk naphthalene vapor densities calculated by equation (3) at the inlet and exit planes of the particular cassette being measured.

Although these results are only meaningfull at regions where fully developed conditions prevailed, they were calculated for cassettes at all duct axial positions, and utilized as a verification of the local results obtained from the coordinate table measurements. This was done by comparing the results from the balance with the local values integrated over the cassette naphthalene surface area. In the vast majority of the data runs, the deviations between these two procedures were around 2.5%, with maximun values of about 6%.

For the mass transfer coefficients already defined, dimensionless mass transfer coefficients were calculated in the form of Sherwood numbers. These are the local Sherwood number

$$Sh_{xy} = (K(x,y)D_h/\nu)\,Sc \qquad (8)$$

and the spanwise-averaged Sherwood number defined as

$$\overline{Sh}(x) = (\bar{K}(x)D_h/\nu)Sc \qquad (9)$$

In equations (7) and (8), D_h is the duct hydraulic diameter

$$D_h = 4wH/(2w + 2H) \qquad (10)$$

and Sc is the Schmidt number. Its value was taken as 2.5 for the naphthalene-air pair, according to [7].

The Reynolds number for the rectangular duct was calculated as

$$Re = 4\dot{W}/(2w + 2H)\mu \qquad (11)$$

where $\dot{W}$ is the air mass flow rate and μ its dynamic viscosity.

RESULTS AND DISCUSSION

The experimental results obtained will be presented in this section in terms of dimensionless mass transfer coefficients. Later in the paper, the analogy between heat and mass transfer will be used to convert these results to heat transfer coefficients.

Spanwise-Averaged Sherwood Numbers. The spanwise-averaged Sherwood numbers, $\overline{Sh}(x)$, will be presented in order to convey information on the development of the transfer coefficients along the duct length. These are plotted in Figures 4, 5 and 6 as functions of the dimensionless axial coordinate, x/D_h, for three values of the duct Reynolds numbers, namely, 10, 20, and 30 thousand. For each value of the Reynolds number, results are displayed for the three values of the tape pitch-to-diameter ratios investigated, as indicated in the legend of the figures. To avoid overlaping of the data for the different values of P/D, the origins of the ordinates of the graphs were displaced, as indicated in the figures. For the middle curves (P/D = 10.3), the ordinate scale is marked at the right side of the figures, as indicated by the arrows. For each set of data corresponding to a particular value of P/D, the distribution of the Sherwood number for the base case related to the Reynolds number in question was also plotted with dark simbols for comparison purposes.

An examination of the figures reveals a common trend in the distribution of the spanwise-averaged Sherwood numbers, for all values of Reynolds numbers and pitch-to-diameter ratios. The spanwise-averaged Sherwood numbers start at a relatively low value at the very entrance of the duct, increasing at an extremely high rate until a maximum value is attained. From this point on, the Sherwood distribution resembles that of a developing flow in a duct, i.e., an initially steep decrease, followed by a moderate rate of decrease, until a constant value characterizing a fully developed condition is reached. The same behavior can be seen in the figures for the base case data. This is an interesting fact since the inlet

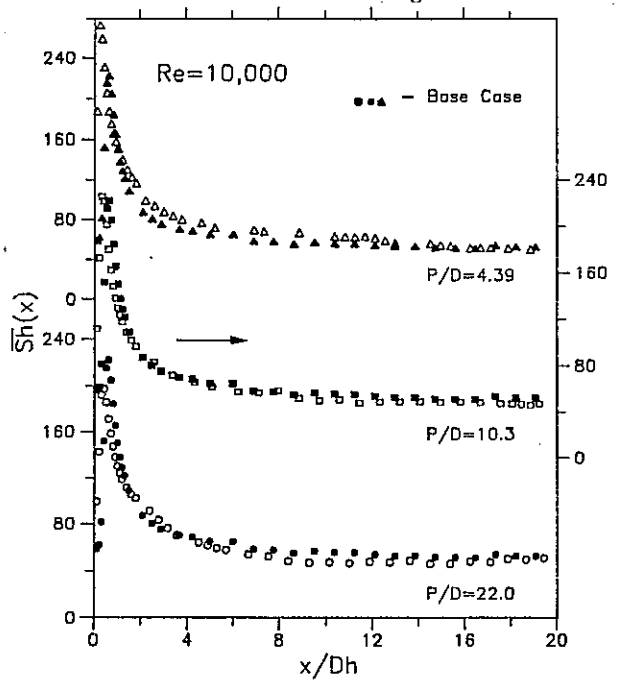

Fig. 4 - Axial distribution of the spanwise-averaged Sherwood number, for $Re = 10000$.

flow conditions for the two cases are totally distinct. The presence of the sharp peak in the spanwise-averaged Sherwood distribution is an indication that a separation zone is also present at the duct entrance for the swirl flow cases, the maximum value corresponding to the reattachment point. This reasoning has been provided before for the base configuration [8].

Figures 4 to 6 also reveal that, in general, the effect of the swirl flow inlet condition on the spanwise-averaged Sherwood numbers in rectangular ducts is surprisingly mild, specially if one recalls the significant enhancements produced by swirl flows in circular geometries [9]. Enhancements of the order of 20-30 percent can be found only for the strongest swirl inlet condition ($P/D = 4.4$), and are limited to regions not too far from the entrance plane ($x/D_h < 5$). These effects are more pronounced for the higher Reynolds numbers. At the end of the duct, the Sherwood numbers for the swirl flow cases tend to the fully developed base case values, indicating that the imposed secondary motions have virtually died away.

Worth noting is the decreasing effect on the spanwise-averaged Sherwood number distribution caused by the utilization of twisted tapes with pitch-to-diameter ratios equal to 10.3. This negative effect occurs in a central region, away from the inlet and exit parts of the duct, and is only clear for the case of $Re = 30,000$, although the decreasing trend is already hinted by the results for the smaller values of Re. Several additional runs were conducted for $P/D = 10.3$, employing both measuring techniques (i.e., balance and local measurements) and the results obtained confirmed the behavior just commented. Further investigation is needed in order to provide a plausible explanation for these results.

Local Sherwood Numbers. Although the spanwise-averaged Sherwood number presentation provides usefull information for design purposes, it masks important characteristics of the flow. The local Sherwood number presentation, on the other hand, furnishes a detailed picture of the flow

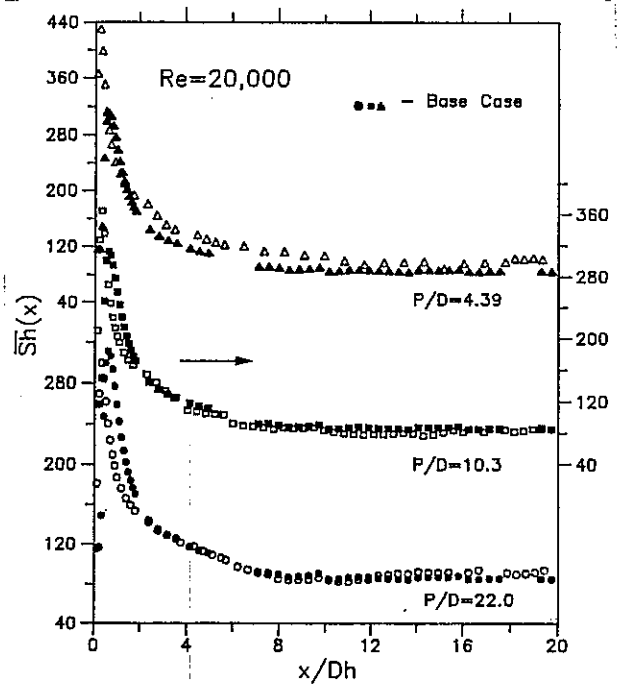

Fig. 5 - Axial distribution of the spanwise-averaged Sherwood number, for $Re = 20000$.

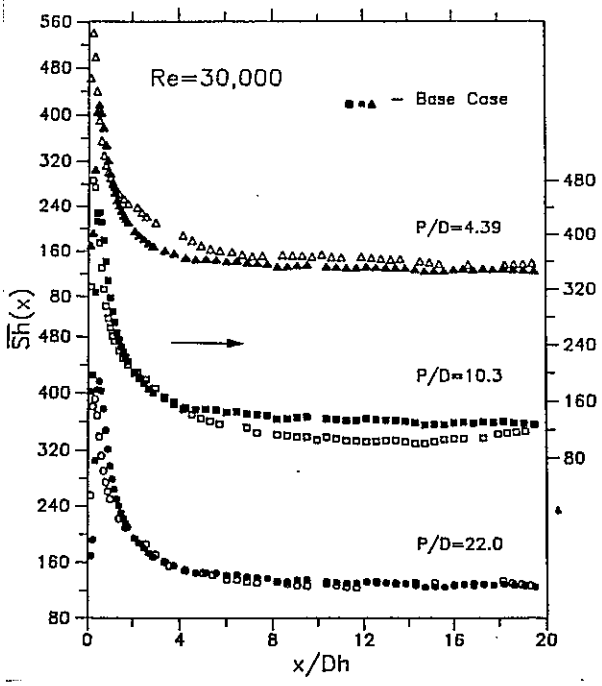

Fig. 6 - Axial distribution of the spanwise-averaged Sherwood number, for $Re = 30000$.

by revealing the points on the surface where mass (heat) transfer is maximum or minimum.

The local Sherwood number distributions are shown in Figures 7-9, for the three values of the Reynolds numbers and tape pitch-to-diameter ratios investigated. In these figures, the ratios of the local Sherwood numbers Sh_{xy} to the base case Sherwood values at the same axial position $\overline{Sh}_b(x)$, are presented as functions of the dimensionless cross stream coordinate, y/w, for the 8 representative axial stations marked along the curves. Table 1 provides the correspondence between the numbers related to each curve and the actual dimensionless axial stations x/D_h.

Several observations can be made by an examination of Figure 7-9. For the case of $Re = 10000$ and $P/D = 4.4$ (Figure 7), it can be seen that the swirl flow inlet condition produces very large values of the local Sherwood number, for certain spanwise locations, at the begining of the duct. Indeed, the local Sherwood values are 2 to 7 times greater than the base case values (i.e., no swirl case) at the same axial position. The local Sherwood distribution peaks at the location where the imposed system of counterrotating vortices pushes *fresh* fluid from the upper part of the duct toward the active wall. This observation can be verified by relating the location of the peaks with the schematic representation of the swirl generating section, displayed at the top of the $P/D = 4.4$ section of the figure in question.

The enhancing effect of the swirl inlet condition is seen to diminishes rapidly as one proceeds downstream into the duct. For instance, at $x/D_h = 1$ (station 3), the peak values in the local Sherwood distribution are no greater than 1.1. For the next axial position, however, the amplitude of the local Sherwood distribution curve is seen to increase relatively to the previous position. This trend is maintained throughout the next two axial stations when a decreasing trend is again verified until the end of the duct. This is a somewhat surprising result since the effect of the swirl flow was expected to continuously decay along the duct length.

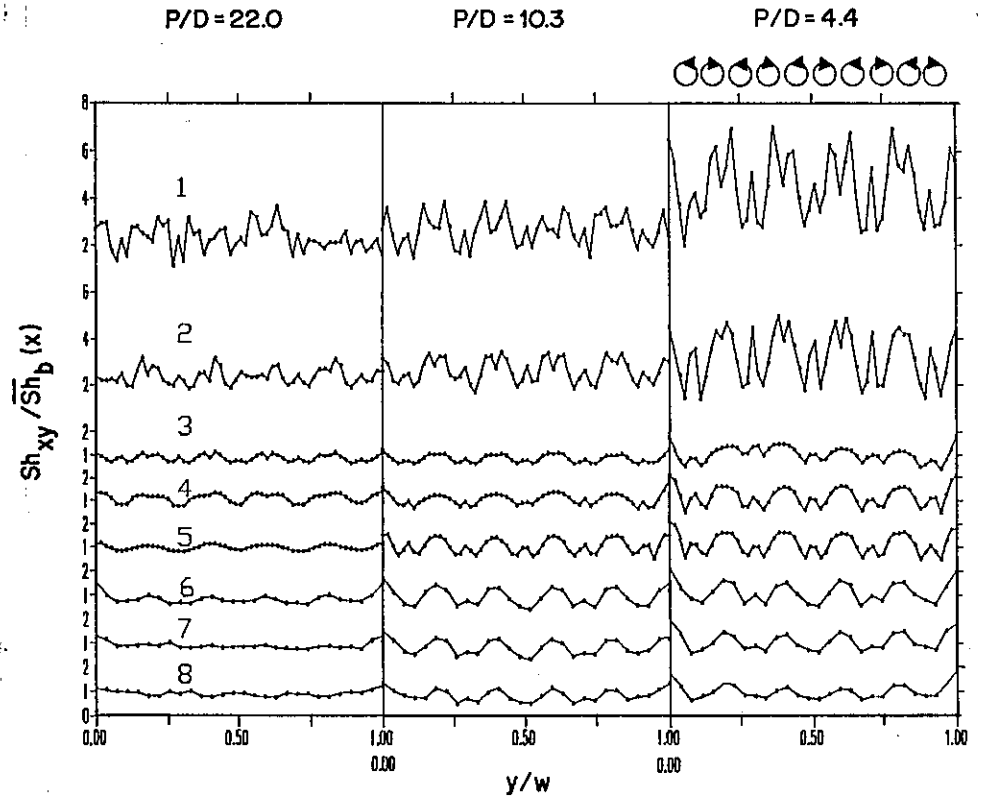

Fig. 7 - Spanwise distribution of the local Sherwood number at different axial stations, for $Re = 10000$.

A possible explanation for the resurgence of the swirl effect can be atributed to streamwise oscilation of the flow. Streamline curvature is known to have an intensifying effect on secondary motions, as a result of Taylor-Gortler instabilities, for concave walls (see Fig. 17.32 (b) of [10]). The same general trends just described for $P/D = 4.4$, are verified for $P/D = 10$ and 22. Figure 8, representing the results for $Re = 20000$, is qualitatively similar to Figure 7. The level of enhancement produced by the swirl flow is not as high as in the previous case, but the swirl resurgence effect is also present.

Smaller, but still significant, enhancing effects at the begining of the duct can be observed in the results presented in Figure 9 for $Re = 30000$. For this value of the Reynolds number, the effect of the swirl flow inlet condition decays continuosly along the duct length until it dies away. No swirl resurgence effect is observed, indicating that the axial oscilation of the main flow mentioned before may not be present or it is not significant.

PRACTICAL SIGNIFICANCE

As mentioned before, the results presented can be used to predict turbulent heat transfer in a rectangular duct of low aspect ratio. The swirl flow inlet condition was shown to augment heat/mass transfer at particular spanwise locations. This constitutes an important information from the application stand point, since it might be used to guide the positioning of critical components with high rates of heat dissipation, in the case of cooling of electronic equipment, or to provide thermal control to hot spots on a heated surface.

The procedure for utilizing the mass transfer results presented in this paper for heat transfer problems is based on the heat-mass transfer analogy, and will be briefly described. The analogy between the heat and mass transfer processes implies that, for the same geometry and flow conditions

$$Nu = f(Re, Pr) \quad \text{and} \quad Sh = f(Re, Sc) \tag{11}$$

Once the relationship between Sh and Re has been experimentally determined (for $Sc = 2.5$), the Nusselt number for the same flow conditions and geometry follows directly from the above equation, for $Pr = 2.5$. For other values of the Prandtl number, however, the results can be extrapolated by utilizing the following relation

$$Nu = \left(\frac{Pr}{Sc}\right)^n Sh \tag{12}$$

with $Sc = 2.5$ for naphthalene experiments. This relation has been quite successful in correlating experimental data for a wide variety of forced-convection flows. For turbulent internal flows, the value of $n = 0.4$ is recommended in the literature [6]. This value however, should be used with caution, since the present flow configuration is highly complex and no heat transfer measurements are available for comparison purposes,

EXPERIMENTAL UNCERTAINTY

An estimate of the uncertainty levels associated to the experimental data obtained was calculated according to the procedure described by Moffat [11]. The data reduction computer program developed incorporated the uncertainty analysis procedure in such a way that every data point reduced was accompanied by an estimate of its experimental uncertainty level.

The typical uncertainty levels to be reported here are

based on the Nth order estimation described by Moffat [11]. For the cassette-averaged results obtained by weighing in the precision balance, uncertainties on the Sherwood numbers were calculated to be in the order of 5 %. For the local measurements, a range of uncertainties of 4 to 10 % was calculated. These values were dependent on the amount of naphthalene sublimed at a particular location. These estimates were verified by the scatter of the values obtained from repeated runs. The analysis revealed that the dominant uncertainty on the experiments was due to the uncertainty on the vapor pressure of the naphthalene at the surface. This information motivated the measurement of the temperature of the naphthalene surface by means of an embeded, pre-calibrated thermocouple.

The uncertainty levels on the Reynolds numbers were calculated to be in the 5-10 % range.

FINAL REMARKS

The present paper investigated the heat transfer characteristics of turbulent swirling flows through a rectangular duct of low aspect ratio. The swirl flow condition was provided by a system of counterrotanting vortices, produced by a vortex generator positioned outside the duct. Local heat transfer results were obtained through the use of the naphthalene sublimation technique in conjuction with the analogy between heat and mass transfer.

The results have shown that very high enhancing effects can be obtained at some positions in the duct by the utilization of the swirl flow inlet condition proposed. The highly complex nature of the flow investigated , however, precluded the presentation of definitive explanations for some of the phenomena observed. In particular, the resurgence of the swirl flow in the duct was documented for some operating conditions, and atributed to streamwise oscilation of the flow. This issue demands further investigation, and can possibly be resolved by flow visualization studies.

Table 1. Dimensionless Axial Positions Presented In Figure 7-9.

Axial Station	x/D_h
1	0.20
2	0.30
3	1.00
4	2.50
5	4.80
6	8.80
7	12.7
8	16.7

NOMENCLATURE

A	cassette exposed naphthalene surface area, m^2
D	internal diameter of swirl generator tube, m
$\mathcal{D}$	naphthalene-air mass diffusivity, m^2/s
D_h	rectangular channel hydraulic diameter, eq. (10), m
H	rectangular channel height, m
K	local mass transfer coefficient, eq. (2), m/s
$\bar{K}$	spanwise-averaged mass transfer coefficient, eq. (5), m/s
$\bar{K}_c$	cassette-averaged mass transfer coefficient, eq. (6), m/s
$\dot{m}''$	mass flux, equation (1), $kg/(m^2 s)$
$\dot{M}''$	spanwise-averaged mass flux, eq. (4), $kg/(m^2 s)$
Δm	cassette-overall mass transfer, kg
P	twisted tape pitch, m
$\dot{Q}$	air volume flow rate, m^3/s
Sc	Schmidt number, $\nu/\mathcal{D}$

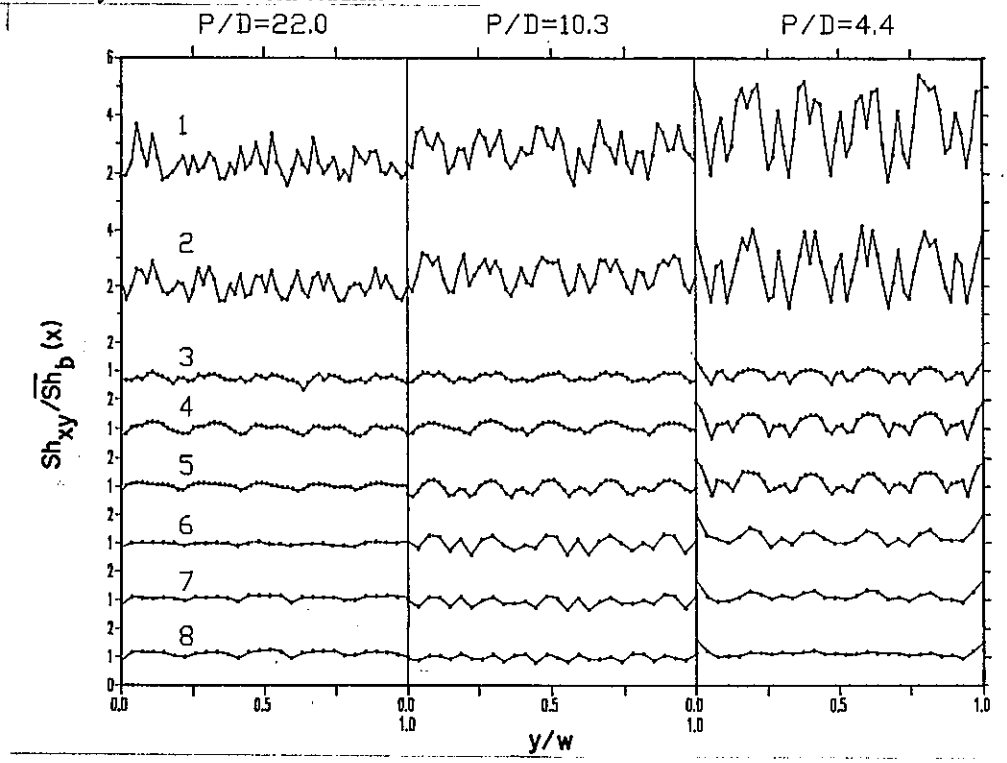

Fig. 8 - Spanwise distribution of the local Sherwood number at different axial stations, for $Re = 20000$.

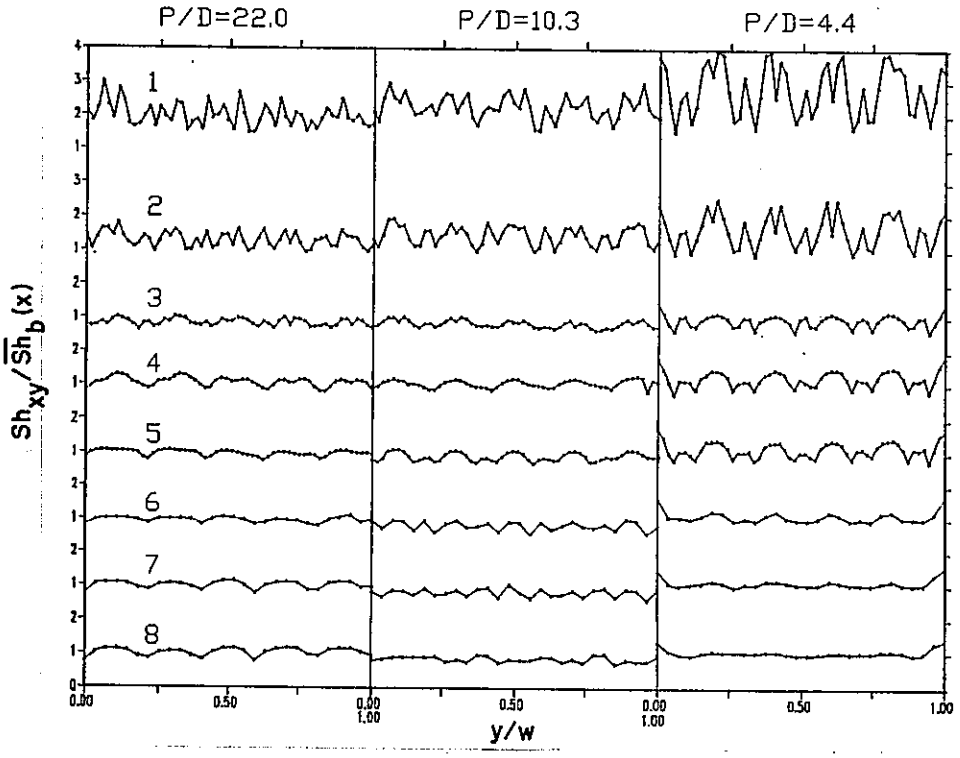

Fig. 9 - Spanwise distribution of the local Sherwood number at different axial stations, for $Re = 30000$.

$\overline{Sh}$	spanwise-averaged Sherwood number, eq. (9)
$\overline{Sh}_b$	base case spanwise-averaged Sherwood number
Sh_{xy}	local Sherwood number, eq. (8)
Δt	time duration of a data run, s
w	width of the rectangular channel, m
$\dot{W}$	air mass flow rate, kg/s
x, y	streamwise and crosstream coordinates, m
δ	sublimation depth, m
μ	air dynamic viscosity, kg/ms
ν	air kinematic viscosity, m^2/s
ρ_{nb}	naphthalene vapor density in the fluid, kg/m^3
ρ_{nw}	naphthalene vapor density at the wall, kg/m^3
ρ_s	density of solid naphthalene, kg/m^3

REFERENCES

1. Goldstein Jr., L., and Sparrow, E., Heat/Mass Transfer Characteristics for Flow in a Corrugated Wall Channel, J. Heat Transfer, 99, 187-195, 1977.
2. Azevedo, L.F.A., and Sparrow, E.M., Natural Convection in Open-Ended Inclined Channels, J. Heat Transfer, 106, 325-332, 1984.
3. Incropera, F.P., Knox, A.L., and Maughan,J.R., Mixed-Convection Flow and Heat Transfer in the Entry Region of a Horizontal Rectangular Duct, J. Heat Transfer, 109, 434-439, 1987.
4. Emery A.F., and Gressner, F.B., The Numerical Prediction of Turbulent Flow and Heat Transfer in the Entrance Region of a Parallel Plate Duct, J. Heat Transfer, 98, 594-600, 1976.
5. Smithberg, E., and Landis, F., Friction and Forced Convection Heat-Transfer Characteristics in Tubes With Twisted Tape Swirl Generators, J. Heat Transfer, 86, 39-49, 1964.
6. Souza Mendes, P.R., The Naphthalene Sublimation Technique, First World Conference on Experimental Heat Transfer, Fluid Mechanics, and Thermodynamics, Dubrovnik, 446-460, 1988.
7. Sogin, H.H., Sublimation From Disks to Air Streams Flowing Normal to Their Surfaces, Trans. ASME, 80, 61-79, 1958.
8. Sparrow, E.M., and Cur, N., Turbulent Heat Transfer in a Symmetrically or Asymmetrically Heated Flat Rectangular Duct With Flow Separation at Inlet, J. Heat Transfer, 104, 82-89, 1982.
9. Sparrow, E.M., and Chaboki, A., Swirl-Affected Turbulent Fluid Flow and Heat Transfer in a Circular Tube, J. Heat Transfer, 106, 766-773, 1984.
10. Schlichting, H., Boundary Layer Theory, Sixth ed., McGraw-Hill, New York, 1968.
11. Moffat, R.J., Contributions to the Theory of Single-Sample Uncertainty Analysis, J. Fluids Engineering, 104, 250-260, 1982.